Exchange interaction in $A\mathrm{Cu_3Fe_2Re_2O_{12}}$ (A = Ca, La, Dy, Na, Cu, Ag, Ce) quadruple perovskites

Fedor Temnikov,[1] Alexey V. Ushakov,[1] Evgenia V. Komleva,[1] Zhehong Liu,[2] Youwen Long,[2] Valentin Yu. Irkhin,[1] and Sergey V. Streltsov[1]

[1]*M. N. Mikheev Institute of Metal Physics, Ural Branch of Russian Academy of Sciences, 620137 Ekaterinburg, Russia*

[2]*Beijing National Laboratory for Condensed Matter Physics, Institute of Physics, Chinese Academy of Sciences, Beijing 100190, China*

(Received 17 June 2025; revised 14 October 2025; accepted 26 November 2025; published 15 December 2025)

Quadruple perovskites $A\mathrm{Cu_3Fe_2Re_2O_{12}}$ attract considerable interest due to their high Curie temperatures (up to 710 K), which strongly depend on the A-site cation. In this work, we employ first-principles calculations to investigate their electronic structure and magnetic exchange interactions. A band mechanism of magnetism that explains the antiferromagnetic character of the exchange interactions and their strong dependence on the filling of the Re t_{2g} states is proposed. These antiferromagnetic interactions stabilize the ferrimagnetic ground state. The calculated Curie temperatures, obtained within the Onsager reaction field theory, are in good agreement with the experimental data.

DOI: 10.1103/k83j-n4h4

I. INTRODUCTION

As a natural generalization of $AB\mathrm{O_3}$ perovskite structures, quadruple perovskites with the chemical formula $AA'_3B_2B'_2\mathrm{O_{12}}$ represent a rich platform that allows for variation in both A- and B-site ions to obtain materials with extraordinary physical properties. In these compounds, the A-site cation is typically a rare-earth, alkali, or alkaline-earth metal with a relatively large ionic radius, while the A' site hosts a Jahn-Teller active transition metal ion, forming square $A'\mathrm{O_4}$ plaquettes. The B and B' sites, which can be occupied by identical or different transition metal ions, are coordinated by oxygen atoms in an octahedral geometry; see Fig. 1. Since A'-, B-, and B'-site ions can all be magnetic, quadruple perovskites may exhibit complex magnetic structures.

Similar to "conventional" $AB\mathrm{O_3}$ perovskites, quadruple perovskites show a variety of different physical phenomena. For example, (Ca, La, or Bi)$\mathrm{Cu_3Mn_4O_{12}}$ exhibit significant low-field magnetoresistance [1–3]. $\mathrm{CaCu_3Ti_4O_{12}}$ is known for its extremely high dielectric constant with weak temperature dependence [4] and has also been proposed as a potential piezoelectric material in the presence of copper vacancies [5]. Ferrimagnetism with relatively high critical temperatures is observed in a series of $R\mathrm{Cu_3Mn_4O_{12}}$, R= rare-earth metal, (T_C up to 400 K) [6,7], as well as in $\mathrm{CaCu_3Cr_2Re_2O_{12}}$ (T_C = 360 K) [8].

Another class of quadruple perovskites characterized by high ferrimagnetic transition temperatures is $A\mathrm{Cu_3Fe_2Re_2O_{12}}$. T_C in these compounds varies over a wide range of 170–710 K [9–12] depending on the A cation. Moreover, first-principles calculations have predicted half-metallic ferrimagnetism in several members of this series, with an energy gap of approximately 2 eV in the nonconducting spin channel [11–13]. This makes $A\mathrm{Cu_3Fe_2Re_2O_{12}}$ an extremely interesting candidate for spin filters, whose efficiency depends on three key parameters: the spin-majority channel gap (which blocks thermally activated conductance), the magnetization (determining spin polarization), and the Curie temperature (defining the operational temperature range) [10].

While impressive progress has been recently achieved in synthesis of such materials as $\mathrm{LaCu_3Fe_2Re_2O_{12}}$ and $\mathrm{DyCu_3Fe_2Re_2O_{12}}$ with T_C = 710 and 650 K, respectively, theoretical understanding is still lacking. In addition to calculations for a few quadruple perovskites [11,12] a possible role of the number of d electrons on Re was suggested [14].

In this paper we studied exchange interaction in $A\mathrm{Cu_3Fe_2Re_2O_{12}}$ by means of *ab initio* calculations. It is shown that these are Cu-Re and Fe-Re exchange interactions which determine magnetic ordering. Interestingly, a naive superexchange model does not seem to explain details of exchange coupling, so we propose a model based on band magnetism. This model naturally explains increase of Curie temperature with the number of Re t_{2g} electrons. The Onsager reaction field theory, which goes beyond the mean-field approximation, reproduces this trend observed experimentally.

II. CALCULATION DETAILS

First-principles density functional theory (DFT) calculations were performed using the Vienna *Ab initio* Simulation Package (VASP) [15] in the generalized gradient approximation [16]. To account for strong on-site electron correlations in the transition metal d states, the GGA + U method in the Dudarev formulation [17] was applied, using the following values of $U - J_H$: 7 eV for Cu [18], 4.1 eV for Fe [19], and 1.5 eV for Re [20].

The energy cutoff is set to 500 eV and the reciprocal space division is $8 \times 8 \times 8k$ points. The experimental crystal structure data for all $A\mathrm{Cu_3Fe_2Re_2O_{12}}$ compounds with the space group $Pn\bar{3}$ (No. 201) reported in [9] (A = Ca), [10] (A = La), [11] (A = Dy), [12] (A = Na), and (A = Cu, Ag, Ce) [21], were used.

Although the electron states in different bands have different degrees of localization, a simple effective Heisenberg model,

$$H = \sum_{i>j} J_{ij}\mathbf{S}_i\mathbf{S}_j, \tag{1}$$

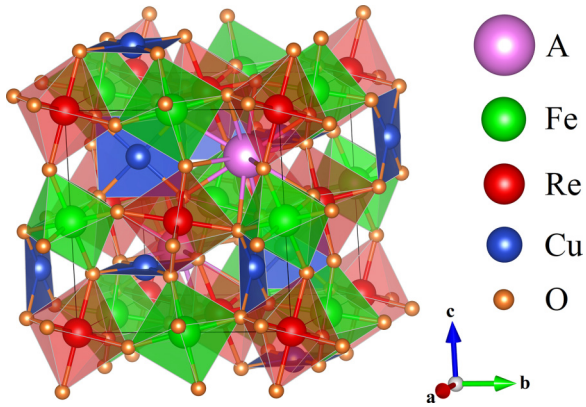

FIG. 1. The crystal structure of $ACu_3Fe_2Re_2O_{12}$ quadruple perovskites.

is a reasonable approximation. Here i and j numerate sites and summation runs once over each index pair. Spins for Cu^{2+} ($S = 1/2$) and Fe^{3+} ($S = 5/2$) are chosen according to their valencies, while for Re we fix $S = 1$ to be able to analyze properties of all materials within the same model. The exchange constants J_{ij} were obtained by the Wannier function projection technique using the Green's function approach [22].

The correctness of the Wannier projection is confirmed by the agreement between the DFT + U band structure and that reconstructed from the Wannier functions; the $NaCu_3Fe_2Re_2O_{12}$ case is shown in Fig. 2. The projection was performed onto the subspace of the O-2p, Cu-3d, Fe-3d, and Re-t_{2g} states. A visualization of the Wannier orbitals corresponding to the exchange parameter $J_{\text{Cu-Re}}$ is presented in Fig. 3.

III. DFT + U RESULTS

A. Electronic structure and origin of half-metallicity

We start by describing the electronic structure of $ACu_3Fe_2Re_2O_{12}$, as it critically influences the magnetic

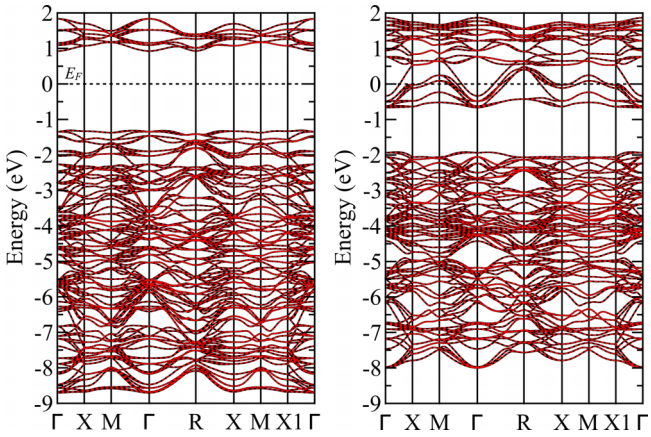

FIG. 2. Band structure comparison of $NaCu_3Fe_2Re_2O_{12}$ obtained by DFT + U calculation. Initial DFT + U bands are shown in black, projected on Wannier functions in red. The left panel illustrates the majority-spin channel, and the right panel, the minority-spin channel.

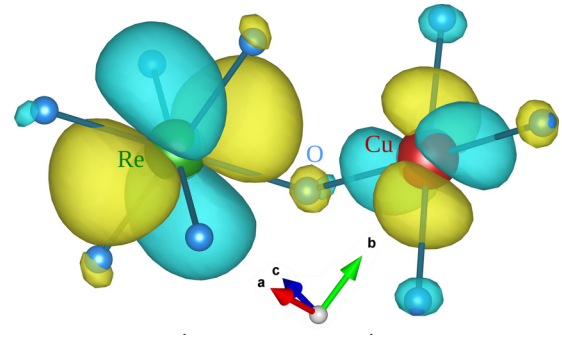

FIG. 3. Wannier orbitals (Cu $x^2 - y^2$ and Re xy) employed for the calculation of the exchange parameter $J_{\text{Cu-Re}}$.

properties. All these materials are half-metals in DFT + U calculations. Figure 4 shows the density of states (DOS) for two representative quadruple perovskites with different numbers of Re t_{2g} electrons.

Strong Hubbard repulsion on Fe, Cu, and the rare-earth element (if present) shifts the 3d (or 4f) states away from the Fermi level. Re 5d (in particular, t_{2g}) bands are much less correlated ($U \sim 1.5 - 2$ eV is of the order of the t_{2g} bandwidth [20,23,24]) and more hybridized with O 2p. Consequently, the system exhibits no Mott gap or well-defined Hubbard bands in DFT + U. Instead, we observe a Stoner-like splitting, with the Fermi level crossing the spin-minority Re t_{2g} band while a gap forms in the spin-majority channel (Re e_g states are at ∼5–

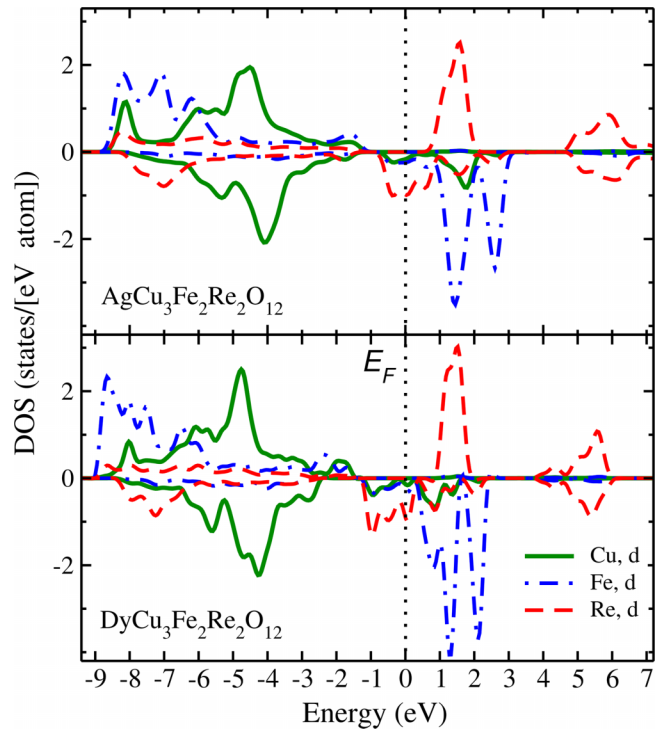

FIG. 4. Density of states (DOS) as obtained in DFT + U calculations. Due to different valences of A ions Re is expected to have $n^{\text{nominal}}_{\text{Re-}d} = 1.5$ or $n = 2.5$ electrons on the t_{2g} shell for Ag and Dy, respectively. Positive (negative) DOS correspond to spin majority (minority).

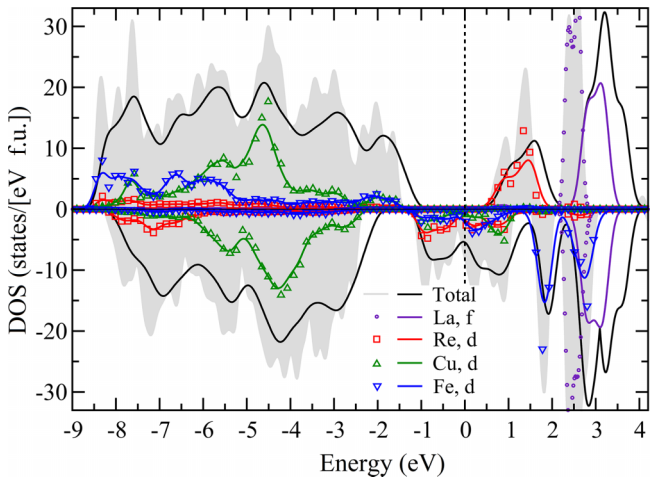

FIG. 5. Density of states (DOS) as obtained in DFT + U (symbols for partial DOS and shaded background for total DOS) and DFT + U + SOC (solid lines) calculations for $LaCu_3Fe_2Re_2O_{12}$.

6 eV). The strong antiferromagnetic (AFM) Fe-Re and Re-Cu exchange interactions, whose mechanism will be discussed below, ensure that all Re ions are ferromagnetically aligned. As a result $ACu_3Fe_2Re_2O_{12}$ materials turn out to be half-metallic on the DFT + U(+SOC) level, while the dynamical correlation effect can potentially modify this situation [13].

Spin-orbit coupling (SOC) playing a minor role in quadruple perovskites despite the fact that Re is a 5d element. SOC leads to a small canting of the Fe and Re magnetic moments [11]. A comparison of the density of states obtained by DFT + U and DFT + U + SOC calculations is presented in Fig. 5 for one of the materials, $LaCu_3Fe_2Re_2O_{12}$. Inclusion of spin-orbit coupling (SOC) leads to a reduction of the band gap in the spin-majority channel by ∼0.4 eV. A noticeable suppression of DOS at the Fermi level is observed. In addition, the La f states are shifted toward higher energies.

B. Magnetic moments

Spin moments, m_s, obtained by DFT + U calculations are summarized in Table I. The magnetic moments on Cu and Fe ions are nearly independent of the A-site ion, indicating that their magnetic states remain unchanged. The moment of the rhenium ion increases with the nominal number of electrons. On average, m_s(Re) is approximately half of the nominal theoretical value, suggesting both a strong hybridization with ligand 2p states and possible itinerant character of rhenium electrons.

TABLE I. Calculated spin moments obtained by the DFT+U method and experimental saturation magnetic moments for $ACu_3Fe_2Re_2O_{12}$ with different A.

A	Cu	Ag	Na	Ca	Dy	La	Ce
m_s(Cu), μ_B	0.6	0.6	0.5	0.6	0.5	0.5	0.5
m_s(Fe), μ_B	4.1	4.1	4.2	4.1	4.1	4.0	4.1
m_s(Re), μ_B	−0.8	−0.8	−0.7	−1.1	−1.3	−1.3	−1.4
$n^{\text{nominal}}_{\text{Re-}d}$	1.5	1.5	1.5	2	2.5	2.5	2.5
$m^{\text{calc}}_{\text{total}}$, μ_B	10.0	10.0	10.0	8.0	16.3[a]	8.0	8.0
$m^{\text{expt}}_{\text{total}}$, μ_B	∼5	–	9.4	8.7	14.0[b]	8.0	8.0

[a]Includes contribution from the A-site ion.
[b]In the field of 7 T, the total magnetic moment is not saturated.

TABLE II. Results of DFT+U calculations for $ACu_3Fe_2Re_2O_{12}$ with different A and experimental T_C. The Heisenberg model is defined in (1) and for Fe^{3+} ($3d^5$) we choose $S = 5/2$, and for Cu^{2+} ($3d^9$) we choose $S = 1/2$; while the number of electrons on Re, $n^{\text{nominal}}_{\text{Re-}d}$, changes in this series for Re, we fix $S = 1$ for convenience. MF stands for mean field (estimation of Curie temperature), and ORF for Onsager reaction field theory (see below, Sec. IV).

	Cu	Ag	Na	Ca	Dy	La	Ce
$J_{\text{Fe-Re}}$ (K)	72	73	40	103	84	73	78
$J_{\text{Fe-Cu}}$ (K)	41	41	23	42	41	24	41
$J_{\text{Cu-Re}}$ (K)	364	356	314	506	530	496	528
$n^{\text{nominal}}_{\text{Re-}d}$	1.5	1.5	1.5	2	2.5	2.5	2.5
T_C^{expt} (K)	200	174	240	560	650	710	625
T_C^{MF} (K)	865	858	675	1246	1197	1122	1170
T_C^{ORF} (K)	444	441	341	641	609	569	594

The total magnetic moments per formula unit obtained from DFT + U calculations are in excellent agreement with the experimental saturation moments for A = La and A = Ce, and small deviations are observed for A = Na and A = Ca. In the case of A = Dy, the theoretical value exceeds the experimental one due to the fact that the full saturation has not been achieved experimentally [11]. A significant difference, approximately by a factor of 2, is observed for the case of $CuCu_3Fe_2Re_2O_{12}$. As shown in Ref. [13], taking into account strong correlations within the DFT + dynamical mean-field theory (DFT+DMFT) approach improves the agreement with experiment, reducing the total magnetic moment to $m^{\text{calc}}_{\text{total}} = 7.6\,\mu_B$. However, the true origin of this discrepancy remains unclear at the moment and further experimental (including possible issues with disorder) and theoretical studies have to be done for this material.

C. Exchange parameters

Results of the exchange interaction of various quadruple perovskites with general chemical formula $ACu_3Fe_2Re_2O_{12}$ are summarized in Table II. One can see that all materials exhibit the same trend: formally the strongest interaction the antiferromagnetic (AFM) Cu-Re exchange $J_{\text{Cu-Re}}$, which is at least 5 times larger than the second-strongest interaction, the AFM Fe–Re coupling $J_{\text{Fe-Re}}$. In fact, these interactions contribute nearly equally to the magnetic energies, if one takes into account different spins of Cu and Fe ions (e.g., energy per Cu-Re bond is 182 K, while it is 180 K per Fe-Re bond in the case of A = Cu). This agrees with the results of a previous theoretical study [14].

The last important exchange coupling is between Fe and Cu ions; it is AFM, but much smaller than $J_{\text{Cu-Re}}$ and $J_{\text{Fe-Re}}$ and cannot override them. As one can see from Fig. 1, these three ions form a Fe-Re-Cu triangles. Therefore, two large

AFM exchanges cause the spins on the remaining bond, Fe-Cu, to be FM.

One clear tendency evident from Table II is the increase in both Cu-Re and Fe-Re exchange interaction strengths with growing electron count on Re, progressing from A = Cu, Ag, Na to Ca, and further to La, Dy, Ce. This tendency is consistent with increasing Curie temperature which is observed experimentally; see T_C^{expt} in Table II. Using the same data from Table II one can calculate that each electron on Re contributes to the exchange energy of $\sim 100 - 130$ K/per bond depending on the material.

D. Exchange mechanism

One might use very different pictures to explain the enhancement of AFM Cu-Re exchange with increasing electron number in the Re 5d shell. In the localized electron picture, this could be interpreted by superexchange mechanism, where the growing number of pathways between half-filled Cu $x^2 - y^2$ and Re t_{2g} orbitals strengthens the interaction (the Re-O-Cu bond angle $\angle \text{Re} - \text{O} - \text{Cu} \approx 110^\circ$ remains nearly constant across all materials).

However, taking advantage of the Green's function method, one can quantitatively evaluate orbital contributions to the total exchange interaction. This analysis reveals that there is a single large element between the Cu $x^2 - y^2$ and Re xy orbitals. Thus, e.g., in $NaCu_3Fe_2Re_2O_{12}$ the main contribution of 312 K due to the Cu $x^2 - y^2$ and Re xy orbitals nearly completely determines the magnitude of the total exchange interaction (314 K) between these two atoms. It has to be also mentioned that the fact that $\angle \text{Re} - \text{O} - \text{Cu}$ strongly deviates from 180° makes overlap between $x^2 - y^2$ and xy orbitals possible.

This suggests that description in terms of band magnetism can be more appropriate to analyze Cu-Re exchange interaction. In Fig. 6 we compare two situations of FM and AFM orders between Cu and Re. Due to the Hubbard repulsion, the $x^2 - y^2$ orbital is half filled and appears slightly above the Fermi energy (at $\sim 1 - 2$ eV according to Fig. 4), while other occupied Cu d states are deep below E_F (at ~ -5 eV). The Re t_{2g} states are exactly at the Fermi level. The hybridization, being possible only for the same spin states, pushes these Re t_{2g} band upward in the FM case and increases the total energy. The situation is just the opposite for the AFM order: hybridization between half-filled Cu spin-up $x^2 - y^2$ and Re spin-up t_{2g} pulls the latter to lower energies and finally results in AFM exchange interaction between Re and Cu. An absolutely equivalent picture can be used to explain AFM coupling for Re and Fe states. We emphasize that this represents only a qualitative model, as quantitative estimates require detailed consideration of the specific band structure in each material.

The band mechanism of AFM coupling has several important implications. First, the energy gain is proportional to the band capacity, i.e., to the number of Re electrons. Furthermore, the same mechanism would contribute to FM coupling, if the t_{2g} band were more than half-filled $n_{\text{Re-}d}^{\text{nominal}} > 3$. Therefore one might expect that maximal AFM exchange interaction is close to the half filling. This agrees with the results of direct DFT + U calculations, see Table II, and experimental observation of the largest Curie temperature

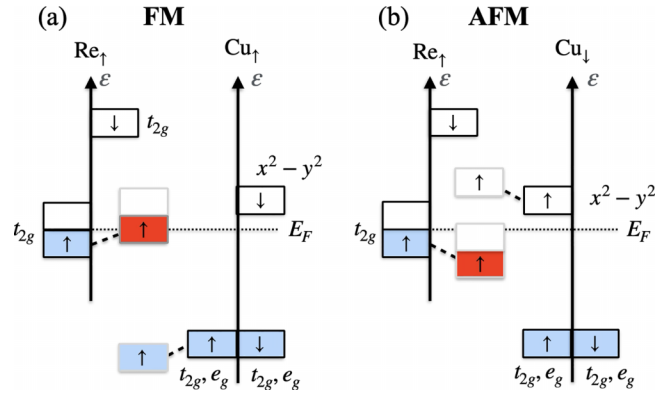

FIG. 6. Sketch of the electronic structure illustrating the mechanism of the antiferromagnetic (AFM) exchange interaction between the metallic Re 5d band crossing the Fermi level and more localized Cu 3d states, which are split due to strong Hubbard's repulsion in such a way that only the $x^2 - y^2$ orbital remains half filled. Hybridization (shown by dashed lines) is allowed only for the states of the same spins. In the case of FM order (a) it shifts the Re 5d band upward, while for (b) AFM order Re 5d states go lower. In the latter case the system gains the exchange energy, and the corresponding coupling turns out to be AFM.

for $LaCu_3Fe_2Re_2O_{12}$ [10] and $DyCu_3Fe_2Re_2O_{12}$ [11] with $n_{\text{Re-}d}^{\text{nominal}} = 2.5$. This also suggests that substituting Re with $Os^{4.5+}$, Ir^{4+}, or similar ions and maintaining other constituents would weaken the AFM Cu-Re and Fe-Re exchange interactions, consequently reducing the Curie temperature.

In order to check the dependence on electron number we performed model calculations artificially changing the position of the Fermi level, when exchange constants are evaluated via the Green's function method. The results are presented in Fig. 7. One can clearly observe suppression of AFM Cu-Re exchange in $DyCu_3Fe_2Re_2O_{12}$ as we move E_F

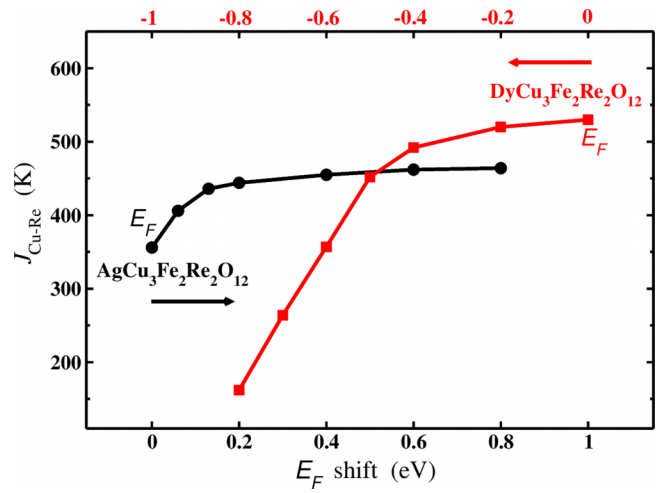

FIG. 7. Results of model calculations of Cu-Re exchange with variation of the Fermi level (Eq. (11) in [22]). For $DyCu_3Fe_2Re_2O_{12}$ (red), shifting E_F to lower energies effectively models a decrease in the number of Re t_{2g} electrons, whereas for $AgCu_3Fe_2Re_2O_{12}$ (black) shifting E_F to higher energies models an increase of the Re t_{2g} occupation. Electronic structure was not recalculated.

TABLE III. Results of DFT+U calculations for $LaCu_3Fe_2Re_2O_{12}$ with different $U^{\text{eff}} = U - J_H$. In each case, U^{eff} for one of the elements was modified, while the other parameters were fixed at default values ($U^{\text{eff}}_{\text{Cu}} = 7$ eV, $U^{\text{eff}}_{\text{Fe}} = 4.1$ eV, $U^{\text{eff}}_{\text{Re}} = 1.5$ eV).

	$U^{\text{eff}}_{\text{Cu}} = 6$ eV	$U^{\text{eff}}_{\text{Cu}} = 7$ eV	$U^{\text{eff}}_{\text{Cu}} = 8$ eV
$J_{\text{Fe-Re}}$ (K)	72	73	83
$J_{\text{Fe-Cu}}$ (K)	18	24	18
$J_{\text{Cu-Re}}$ (K)	476	496	518
T_C^{MF} (K)	1094	1122	1213
T_C^{ORF} (K)	555	569	618
	$U^{\text{eff}}_{\text{Fe}} = 3.1$ eV	$U^{\text{eff}}_{\text{Fe}} = 4.1$ eV	$U^{\text{eff}}_{\text{Fe}} = 5.1$ eV
$J_{\text{Fe-Re}}$ (K)	81	73	81
$J_{\text{Fe-Cu}}$ (K)	14	24	18
$J_{\text{Cu-Re}}$ (K)	486	496	512
T_C^{MF} (K)	1158	1122	1194
T_C^{ORF} (K)	590	569	608
	$U^{\text{eff}}_{\text{Re}} = 1$ eV	$U^{\text{eff}}_{\text{Re}} = 1.5$ eV	$U^{\text{eff}}_{\text{Re}} = 2$ eV
$J_{\text{Fe-Re}}$ (K)	70	73	80
$J_{\text{Fe-Cu}}$ (K)	14	24	22
$J_{\text{Cu-Re}}$ (K)	456	496	532
T_C^{MF} (K)	1057	1122	1217
T_C^{ORF} (K)	538	569	618

downward reducing the number of Re t_{2g} electrons. Interestingly, Fig. 4 shows that the difference in position of the Fermi level between $A =$ Dy and Ag is ∼0.6 eV. Shifting E_F by 0.6 eV (to lower energies) in $DyCu_3Fe_2Re_2O_{12}$ we obtain $J_{\text{Cu-Re}} \sim 360$ K, which is very close to the results of direct calculations for $AgCu_3Fe_2Re_2O_{12}$. Moreover, we observe the opposite tendency of increasing exchange interaction starting from $AgCu_3Fe_2Re_2O_{12}$, where $n^{\text{nominal}}_{\text{Re-}d} = 1.5$ and is now shifting E_F upward. Thus our model calculation clearly demonstrates strong dependence of the exchange interaction on the number of Re t_{2g} electrons. Surprisingly, the account of this factor only is enough to explain suppression of exchange interaction (and consequently T_C) going from $DyCu_3Fe_2Re_2O_{12}$ to $AgCu_3Fe_2Re_2O_{12}$, but $J_{\text{Cu-Re}}$ dependence on the electron number of Re is not linear according to these calculations.

Finally, we performed calculations for a quadruple perovskite containing Os instead of Re: $CuCu_3Fe_2Os_2O_{12}$. There are two types of Cu ions. Those (three Cu per formula unit) occupying CuO_4 plaquettes have a 2+ valence state, while the one in the icosahedral oxygen O_{12} cage is 1+, similar to $CuCu_3Fe_2Re_2O_{12}$ [13,25]. This gives a 5.5+ oxidation state and $n^{\text{nominal}}_{\text{Os-}d} = 2.5$ for Os. $U - J_H = 1.5$ eV for Os is the same as for Re. Calculation of exchange interaction leads to $J_{\text{Cu-Os}} = 520$ K and $J_{\text{Fe-Os}} = 85$ K (suggesting $S = 1$ for Os), which is very similar to what we had in $LaCu_3Fe_2Re_2O_{12}$ and $DyCu_3Fe_2Re_2O_{12}$ with $n^{\text{nominal}}_{\text{Re-}d} = 2.5$.

It is also worth mentioning that calculated exchanges do not strongly depend on choice of Hubbard repulsion (see Table III). Even increasing $U^{\text{eff}} = U - J_H$ on the Re ion from 1 eV to 2 eV changes $J_{\text{Cu-Re}}$ by less than 20%.

IV. ESTIMATION OF CRITICAL TEMPERATURES

Having calculated the exchange constants, one can estimate the Curie temperatures. The simplest way to calculate magnetic properties is via the mean-field approach. For each sublattice a the magnetization in the field H per unit cell (containing n_a atoms of the sort a) is given by

$$M_a = n_a \langle S^z_a \rangle = n_a S_a B_{S_a}\left(\frac{S_a H'_a}{T}\right), \tag{2}$$

where

$$H'_a = H - \sum_b z_{ab} J_{ab} M_b / n_b. \tag{3}$$

B_S is the Brillouin function; z_{ab} is the number of nearest neighbors in the sublattice b of an atom in the sublattice a. Expanding for a small H' and introducing $S_a(S_a + 1) = \mu_a^2$ we obtain

$$M_a = \chi_a^{(0)}(H - \sum_b z_{ab} J_{ab} M_b / n_b), \tag{4}$$

where

$$\chi_a^{(0)} = n_a \mu_a^2 / 3T. \tag{5}$$

Dividing by H we obtain the system of equations for partial susceptibilities of each sublattice, $\chi_a = M_a/H$,

$$\chi_a = \chi_a^{(0)} - \sum_b J_{ab}(0) \chi_a^{(0)} \chi_b / (n_a n_b), \tag{6}$$

where $J_{ab}(0) = J_{ab}(\mathbf{q} = 0) = z_{ab} n_a J_{ab}$, $z_{ab} n_a = z_{ba} n_b$ being the number of exchange-coupled pairs.

From the high-temperature expansion for the total susceptibility $\chi = \sum_a n_a \chi_a$, the paramagnetic Curie-Weiss temperature is given by

$$\theta = -\frac{1}{3} \sum_{a>b} J_{ab}(0) \mu_a^2 \mu_b^2 \Big/ \sum_a n_a \mu_a^2 \tag{7}$$

and is negative for a ferrimagnet with antiferromagnetic exchange interactions [$J_{ab}(0) > 0$].

The condition for the determinant

$$\left| 1 + J_{ab}(0) \chi_a^{(0)} \big/ (n_a n_b) \right| = 0 \tag{8}$$

with susceptibility $\chi_a^{(0)}$ depending on temperatures gives us the Curie temperature. For quadruple perovskites we can use a three-sublattice model with exchange parameters between sublattices only, the first sublattice corresponding to Fe ions, the second to Re ions, and the third to Cu ions. In this case one obtains the cubic equation for T_C in the following standard form:

$$T_C^3 + p T_C + q = 0, \tag{9}$$

where

$$p = -\left(\tilde{J}_{12}^2 + \tilde{J}_{13}^2 + \tilde{J}_{23}^2\right),$$
$$q = 2 \tilde{J}_{12} \tilde{J}_{13} \tilde{J}_{23}, \tag{10}$$

and $\tilde{J}_{ab} = \frac{1}{3} \mu_a \mu_b J_{ab}(0) / \sqrt{n_a n_b}$. Since the arithmetic mean is greater than or equal to the geometric mean, we have

$$Q = \left(\frac{p}{3}\right)^3 + \left(\frac{q}{2}\right)^2 \leqslant 0. \tag{11}$$

Then the solution of the cubic equation is obtained by the trigonometric substitution:

$$T_C = 2\sqrt{-\frac{p}{3}}\cos\left[\frac{1}{3}\arccos\left(\frac{3q}{2p}\sqrt{\frac{-3}{p}}\right)\right]. \quad (12)$$

If we neglect exchange interaction between Fe and Cu, $J_{13} = 0$, T_C is given by

$$T_C = \sqrt{\tilde{J}_{12}^2 + \tilde{J}_{23}^2} = \frac{1}{3}\mu_2\sqrt{\frac{\mu_1^2 J_{12}^2(0)}{n_1 n_2} + \frac{\mu_3^2 J_{23}^2(0)}{n_2 n_3}}. \quad (13)$$

To take into account a possible partial itinerancy of electrons, the mean-field approach can be modified by generalizing the Heisenberg model to an effective interpolating model [26]. Then the moments μ_a may become noninteger being renormalized due to electron delocalization.

To take into account fluctuation effects, we can use the Onsager reaction field (ORF) theory which is equivalent to the random-phase approximation and similar to the Tyablikov approach [27]. For simplicity, we calculated the Onsager renormalization (see Table II) by taking into account two main exchange parameters only, $J_{12} = J_{\text{Fe-Re}}$ and $J_{23} = J_{\text{Re-Cu}}$, and putting $J_{13} = 0$. Then the renormalized T_C is given by $T_C = T_C^{(0)}/I$ with the renormalization factor,

$$I = \sum_{\mathbf{q}} \frac{\tilde{J}_{12}^2(0) + \tilde{J}_{23}^2(0)}{\tilde{J}_{12}^2(0) - \tilde{J}_{12}^2(\mathbf{q}) + \tilde{J}_{23}^2(0) - \tilde{J}_{23}^2(\mathbf{q})}. \quad (14)$$

Here $T_C^{(0)}$ is the Curie temperature in the mean-field approximation, e.g., (13), and q dependencies of exchange integrals for this particular lattice are

$$J_{12}(\mathbf{q}) = 4J_{12}\left(3 + \cos\left(\frac{q_x a}{2}\right) + \cos\left(\frac{q_y a}{2}\right) + \cos\left(\frac{q_z a}{2}\right)\right),$$

$$\begin{aligned} J_{23}(\mathbf{q}) = J_{23}\Bigg(&9 + 3\cos\left(\frac{q_x a}{4} + \frac{q_y a}{4} + \frac{q_z a}{4}\right) \\ &+ 4\cos\left(\frac{q_x a}{4} - \frac{q_y a}{4} + \frac{q_z a}{4}\right) \\ &+ 4\cos\left(\frac{q_x a}{4} + \frac{q_y a}{4} - \frac{q_z a}{4}\right) \\ &+ 4\cos\left(\frac{q_x a}{4} - \frac{q_y a}{4} - \frac{q_z a}{4}\right)\Bigg). \end{aligned} \quad (15)$$

In Table II we present renormalized Curie temperatures for all studied materials. Interestingly, the renormalization factor varies only weakly, from $I = 1.91$ to 1.98. The calculations demonstrate good overall agreement with the experimental Curie temperatures, further supporting the correctness of the exchange parameters obtained via the DFT + U method and the analysis performed using this approach.

V. CONCLUSIONS

In this paper, we investigated the electronic structure and magnetic interactions in the quadruple perovskites $A\text{Cu}_3\text{Fe}_2\text{Re}_2\text{O}_{12}$ using DFT + U calculations and estimated Curie temperatures in the mean-field approach and Onsager reaction field theory. All the compounds were found to be half-metallic within DFT + U due to Stoner-like splitting of delocalized Re 5d states and strong on-site Hubbard repulsion of localized Fe and Cu 3d electrons. The magnetic structure is determined by strong antiferromagnetic exchange interactions between Re-Cu and Re-Fe which lead to the ferrimagnetic ground state. While Cu and Fe moments are ferromagnetically aligned, conducting Re t_{2g} states reside in the spin-minority channel.

Although all these compounds have similar magnetic properties, there are notable differences. The A = Ca, La, Dy, and Ce systems have high T_C, DFT + U calculations confirming the large exchange parameter for these compounds. On the other hand, A = Cu, Ag, and Na compounds have lower T_C, which is consistent with the smaller calculated exchange interactions. Besides that, the experimental value of the magnetic moment for $\text{CuCu}_3\text{Fe}_2\text{Re}_2\text{O}_{12}$ is strongly reduced. As demonstrated in Ref. [13], this may indicate violation of half-metallicity owing to strong correlation effects.

We propose a band mechanism to explain the nature and strength of Cu-Re and Fe-Re exchange interactions. Our calculations confirm partially itinerant features of rhenium d-electrons suggested previously; a strong dependence of the exchange interactions on their number is demonstrated. Calculations for A = Cu, Ag, and Na yield considerably reduced Re magnetic moments. The reduction in the number of d electrons on Re, caused by substituting the A-site cation from A^{3+} to A^{2+} and A^{1+}, decreases the occupancy of the Re t_{2g} states below the Fermi level. This, in turn, reduces the exchange interaction strength and consequently lowers T_C. Furthermore, model calculations demonstrate that shifting the Fermi level results in a similar effect, so the quadruple perovskites $A\text{Cu}_3\text{Fe}_2\text{Re}_2\text{O}_{12}$ demonstrate both localized-spin (Fe and Cu) and itinerant features (Re) in magnetism.

Theoretical values of T_C based on calculated exchange parameters significantly overestimate the experimental T_C values in the mean-field approach. Tyablikov-Onsager renormalization provides a satisfactory agreement, but overestimates T_C for A = Ag and Cu. $\text{CuCu}_3\text{Fe}_2\text{Re}_2\text{O}_{12}$ stands out as the most exotic material among all studied quadruple perovskites with experimentally observed low saturation magnetization and anharmonic specific heat [13]. Consequently, it is unsurprising that simple DFT + U calculations fail to achieve perfect agreement with experiment. This discrepancy arises from two main factors: first, the added complexity of rattling Cu ions in an icosahedral coordination [25] and, second, the significant role of many-body effects, as revealed by DMFT calculations. They result in a substantial reconstruction of the electronic structure, suppressing the half-metallic state [13], which in turn can renormalize the exchange interactions.

ACKNOWLEDGMENTS

The first-principles calculations were supported by the Russian Science Foundation via Project No. RSF 23-42-00069, while estimation of the Curie temperature by Onsager reaction field theory was performed with support by the Ministry of Science and Higher Education of the Russian

Federation. Y.L. and Z.L. were supported by the National Key R&D Program of China (Grant No. 2021YFA1400300), and the National Natural Science Foundation of China (Grants No. 12425403, No. 12261131499, and No. 12204516).

DATA AVAILABILITY

The data that support the findings of this article are not publicly available. The data are available from the authors upon reasonable request.

[1] Z. Zeng, M. Greenblatt, M. A. Subramanian, and M. Croft, Large low-field magnetoresistance in perovskite-type $CaCu_3Mn_4O_{12}$ without double exchange, Phys. Rev. Lett. **82**, 3164 (1999).

[2] J. Alonso, J. Sánchez-Benıtez, A. De Andrés, M. Martınez-Lope, M. Casais, and J. Martınez, Enhanced magnetoresistance in the complex perovskite $LaCu_3Mn_4O_{12}$, Appl. Phys. Lett. **83**, 2623 (2003).

[3] K. Takata, I. Yamada, M. Azuma, M. Takano, and Y. Shimakawa, Magnetoresistance and electronic structure of the half-metallic ferrimagnet $BiCu_3Mn_4O_{12}$, Phys. Rev. B **76**, 024429 (2007).

[4] A. Ramirez, M. Subramanian, M. Gardel, G. Blumberg, D. Li, T. Vogt, and S. Shapiro, Giant dielectric constant response in a copper-titanate, Solid State Commun. **115**, 217 (2000).

[5] K. Wang, X. Guo, C. Han, L. Liu, Z. Wang, L. Thomsen, P. Chen, Z. Shao, X. Wang, F. Xie *et al.*, Creation of piezoelectricity in quadruple perovskite oxides by harnessing cation defects and their application in piezo-photocatalysis, ACS Nano **19**, 3818 (2025).

[6] J. Sánchez-Benítez, J. Alonso, H. Falcón, M. Martínez-Lope, A. De Andrés, and M. Fernández-Díaz, Preparation under high pressures and neutron diffraction study of new ferromagnetic $RCu_3Mn_4O_{12}$ (R = Pr, sm, eu, gd, dy, ho, tm, yb) perovskites, J. Phys.: Condens. Matter **17**, S3063 (2005).

[7] J. Sanchez-Benitez, J. A. Alonso, M. J. Martínez-Lope, A. de Andres, and M. T. Fernández-Díaz, Enhancement of the curie temperature along the perovskite series $RCu_3Mn_4O_{12}$ driven by chemical pressure of R^{3+} cations (mR = rare earths), Inorg. Chem. **49**, 5679 (2010).

[8] J. Zhang, Z. Liu, X. Ye, X. Wang, D. Lu, H. Zhao, M. Pi, C.-T. Chen, J.-L. Chen, C.-Y. Kuo *et al.*, High-pressure synthesis of quadruple perovskite oxide $CaCu_3Cr_2Re_2O_{12}$ with a high ferrimagnetic curie temperature, Inorg. Chem. **63**, 3499 (2024).

[9] W.-t. Chen, M. Mizumaki, H. Seki, M. S. Senn, T. Saito, D. Kan, J. P. Attfield, and Y. Shimakawa, A half-metallic a-and b-site-ordered quadruple perovskite oxide $CaCu_3Fe_2Re_2O_{12}$ with large magnetization and a high transition temperature, Nat. Commun. **5**, 3909 (2014).

[10] Z. Liu, S. Zhang, X. Wang, X. Ye, S. Qin, X. Shen, D. Lu, J. Dai, Y. Cao, K. Chen, F. Radu, W.-B. Wu, C.-T. Chen, S. Francoual, J. R. L. Mardegan, O. Leupold, L. H. Tjeng, Z. Hu, Y.-f. Yang, and Y. Long, Realization of a half metal with a record-high curie temperature in perovskite oxides, Adv. Mater. **34**, 2200626 (2022).

[11] Z. Liu, J. Peng, X. Wang, F. Temnikov, A. Ushakov, X. Ye, Z. Pan, J. Zhang, M. Pi, S. Tang, K. Chen, F. Radu, Z. Hu, C.-T. Chen, Z. Chi, Z. Pchelkina, V. Irkhin, Y. Shen, S. V. Streltsov, and Y. Long, High-pressure synthesis and high-performance half metallicity of quadruple perovskite oxide $DyCu_3Fe_2Re_2O_{12}$, Fundam. Res. (2024).

[12] J. Zhang, F. Temnikov, X. Ye, X. Wang, Z. Pan, Z. Liu, M. Pi, S. Tang, C.-T. Chen, C.-W. Pao *et al.*, Large manipulation of ferrimagnetic curie temperature by a-site chemical substitution in $ACu_3Fe_2Re_2O_{12}$ (A = Na, ca, and la) half metals, Inorg. Chem. **64**, 472 (2025).

[13] A. I. Poteryaev, Z. V. Pchelkina, S. V. Streltsov, Y. Long, and V. Yu. Irkhin, Highly correlated electronic state in the ferrimagnetic quadruple perovskite $CuCu_3Fe_2Re_2O_{12}$, JETP Lett. **121**, 67 (2025).

[14] D. Wang, M. Shaikh, S. Ghosh, and B. Sanyal, Prediction of half-metallic ferrimagnetic quadruple perovskites $ACu_3Fe_2Re_2O_{12}$ (A = Ca, sr, ba, pb, sc, Y, la) with high curie temperatures, Phys. Rev. Mater. **5**, 054405 (2021).

[15] G. Kresse and J. Furthmüller, Efficient iterative schemes for *ab initio* total-energy calculations using a plane-wave basis set, Phys. Rev. B **54**, 11169 (1996).

[16] J. P. Perdew, K. Burke, and M. Ernzerhof, Generalized gradient approximation made simple, Phys. Rev. Lett. **77**, 3865 (1996).

[17] S. L. Dudarev, G. A. Botton, S. Y. Savrasov, C. J. Humphreys, and A. P. Sutton, Electron-energy-loss spectra and the structural stability of nickel oxide: An LSDA+U study, Phys. Rev. B **57**, 1505 (1998).

[18] L. Sun, J. Han, Q. Ge, X. Zhu, and H. Wang, Understanding the role of Cu^+/Cu^0 sites at Cu_2O based catalysts in ethanol production from CO_2 electroreduction—A DFT study, RSC Adv. **12**, 19394 (2022).

[19] J. Hong, A. Stroppa, J. Íniguez, S. Picozzi, and D. Vanderbilt, Spin-phonon coupling effects in transition-metal perovskites: A DFT+U and hybrid-functional study, Phys. Rev. B **85**, 054417 (2012).

[20] T.-W. Lim, S.-D. Kim, K.-D. Sung, Y.-M. Rhyim, H. Jeen, J. Yun, K.-H. Kim, K.-M. Song, S. Lee, S.-Y. Chung *et al.*, Insights into cationic ordering in re-based double perovskite oxides, Sci. Rep. **6**, 19746 (2016).

[21] Y. Long *et al.* (unpublished).

[22] D. M. Korotin, V. V. Mazurenko, V. I. Anisimov, and S. V. Streltsov, Calculation of exchange constants of the heisenberg model in plane-wave-based methods using the Green's function approach, Phys. Rev. B **91**, 224405 (2015).

[23] H.-S. Kim and H.-Y. Kee, Crystal structure and magnetism in α-$RuCl_3$: An *ab initio* study, Phys. Rev. B **93**, 155143 (2016).

[24] M. R. Scudder, B. He, Y. Wang, A. Rai, D. G. Cahill, W. Windl, J. P. Heremans, and J. E. Goldberger, Highly efficient transverse thermoelectric devices with Re_4Si_7 crystals, Energy Environ. Sci. **14**, 4009 (2021).

[25] Z. V. Pchelkina, E. V. Komleva, V. Yu. Irkhin, Y. Long, and S. V. Streltsov, Rattling phonon modes in quadruple perovskites, JETP Lett. **118**, 738 (2023).

[26] A. L. Wysocki, J. K. Glasbrenner, and K. D. Belashchenko, Thermodynamics of itinerant magnets in a classical spin-fluctuation model, Phys. Rev. B **78**, 184419 (2008).

[27] G. Wysin, Onsager reaction-field theory for magnetic models on diamond and hcp lattices, Phys. Rev. B **62**, 3251 (2000).